Neurotherapeutics (2012) 9:210–225
DOI 10.1007/s13311-011-0084-7

ORIGINAL ARTICLE

Glucocorticoid-Induced Leucine Zipper (GILZ) Over-Expression in T Lymphocytes Inhibits Inflammation and Tissue Damage in Spinal Cord Injury

Emanuela Esposito · Stefano Bruscoli · Emanuela Mazzon · Irene Paterniti · Maddalena Coppo · Enrico Velardi · Salvatore Cuzzocrea · Carlo Riccardi

Published online: 29 November 2011
© The American Society for Experimental NeuroTherapeutics, Inc. 2011

Abstract Spinal cord injury (SCI) is a traumatic event that causes a secondary and extended inflammation characterized by infiltration of immune cells, including T lymphocytes, release of pro-inflammatory mediators in the lesion site, and tissue degeneration. Current therapeutic approaches for SCI are limited to glucocorticoids (GC) due to their potent anti-inflammatory activity. GC efficacy resides, in part, in the capability to inhibit NF-κB, T lymphocyte activation, and the consequent cytokine production. In this study, we performed experiments aimed to test the susceptibility of glucocorticoid-induced leucine zipper (GILZ) transgenic ($GILZ^{TG}$) mice, in which GILZ is selectively over-expressed in T lymphocytes, to SCI induction. Consistent with a decreased inflammatory response, $GILZ^{TG}$ were less susceptible to SCI as compared to wild-type littermates. Notably, inhibition of NF-κB activation and nuclear translocation, diminished T lymphocytes activation and tissue infiltration, as well as decreased release of cytokines were evident in $GILZ^{TG}$ as compared to wild-type mice. Moreover, $GILZ^{TG}$ showed a reduced tumor necrosis factor-α, IL-1β, Inductible nitric oxide synthase (iNOS) and nytrotyrosine production, apoptosis, and neuronal tissue damage. Together these results indicate that GILZ mimics the anti-inflammatory effect of GC and represents a potential pharmacological target for modulation of T lymphocyte-mediated immune response in inflammatory disorders, such as SCI.

Keywords Glucocorticoid-induced leucine zipper · glucocorticoids · T lymphocytes · inflammation · spinal cord injury · apoptosis

Introduction

Inflammation is involved in a large array of pathological conditions as a homeostatic response aimed at tissue repair and to defend organ functional integrity. Many signals and stimuli (including traumatic events) are responsible for the inflammatory process activation and development [1]. A post-traumatic inflammatory reaction plays an important role in the secondary injury process that develops after spinal cord injury (SCI) [2]. The primary traumatic mechanical injury to the spinal cord causes the death of a number of neurons that can neither be recovered nor regenerated. However, neurons continue to die for hours after SCI and this represents a potentially avoidable event [3]. In particular, this secondary neuronal death is determined by a large number of cellular and molecular events (characteristic of local inflammatory response) that have been proposed to contribute significantly to secondary damage in the injured spinal cord. Recent evidence suggests that leukocytes, especially T lymphocytes and neutrophils, infiltrate into the injured spinal cord and are directly involved in the pathogenesis and extension of SCI

E. Esposito and S. Bruscoli contributed equally to this article.

Electronic supplementary material The online version of this article (doi:10.1007/s13311-011-0084-7) contains supplementary material, which is available to authorized users.

E. Esposito · E. Mazzon · I. Paterniti · S. Cuzzocrea (✉)
Department of Clinical and Experimental Medicine and Pharmacology, School of Medicine, University of Messina, Torre Biologica, Policlinico Universitario Via C. Valeria, Gazzi, 98125 Messina, Italy
e-mail: salvator@unime.it

S. Bruscoli · M. Coppo · E. Velardi · C. Riccardi (✉)
Department of Clinical and Experimental Medicine, Section of Pharmacology, Tossicology and Chemioterapy, University of Perugia, Via del Giochetto, 06122 Perugia, Italy
e-mail: riccardi@unipg.it

[4–6]. Moreover, relevant features of inflammation, such as inflammatory cells infiltration, inflammatory mediators release, edema formation, neuronal apoptosis, and tissue damage have been characterized in SCI animal models [7, 8].

Despite progress, SCI still remains a very complex medical and psychological challenge, and the only pharmacological compound that has been recognized as therapeutically useful is the synthetic glucocorticoid (GC) methylprednisolone (MP), when administered at high doses within 3 to 8 hours from the onset of the trauma [9]. The use of GC in the treatment of SCI has been proposed on the basis of the ability of high-dose MP to attenuate posttraumatic free radical-induced lipid peroxidation [10] or attenuation of oligodendrocyte apoptosis after injury [11]. However, the mechanisms by which GC protect the central nervous system are not completely understood. Some studies suggest that GC-mediated neuroprotetion in central nervous system diseases, such as the Parkinson's disease is due to the anti-inflammatory properties of GC [12]. Among the most used drugs for treatment of SCI patients, GC exerts the anti-inflammatory action through inhibition of T-lymphocyte activation and migration, entering into the lesion of the tissue and production of pro-inflammatory cytokines. These effects are mediated by GC interaction with cytoplasm receptors, which is followed by the inhibition of NF-κB activation and nuclear translocation [13, 14]. However, although GC is a potent anti-inflammatory drug, its clinical effects are often transitory, and the disease recurs when tapering the drug and when chronic use of GC is accompanied by serious side effects. Therefore, different strategies aimed to inhibit the NF-κB-mediated inflammation are needed.

We have previously identified a gene known as glucocorticoid-induced leucine zipper (GILZ), which is rapidly activated by dexamethasone (DEX), a synthetic GC specific for GR, and inhibits T-lymphocyte activation [15, 16]. The GILZ gene encodes various isoforms among which GILZ is the isoform expressed in normal T lymphocytes that mediates some of the immunomodulatory effects of GC, including inhibition of NF-κB activation and nuclear translocation [15–21]. Notably, GILZ directly interacts with NF-κB in a homodimeric conformation through specific amino acids at the COOH terminal domain [21]. Moreover, GILZ can interact with Ras-dependent mitogen activated protein kinase pathway, in a monomeric conformation and through its NH2 terminal domain, with consequent inhibition of the downstream pathways, including NF-κB activation [22]. Thus, GILZ inhibits NF-κB by multiple mechanisms and acts as an anti-inflammatory molecule [15, 20–24].

Using GILZ transgenic ($GILZ^{TG}$) mice, in which GILZ is selectively over-expressed in the T-cell lineage at levels comparable to that induced by pharmacological GC treatment [20, 25], we show that GILZ inhibits the inflammatory process and the development of SCI. These results indicate that GILZ is an anti-inflammatory molecule representing a potential pharmacological target for modulation of T-cell-mediated immune/inflammatory response in SCI.

Methods

Animals

Six- to 10-week-old $GILZ^{TG}$ and wild-type (WT) mice were used and analyzed for genotype and GILZ expression, as previously described [24]. In each experiment, $GILZ^{TG}$ mice were compared with WT littermates. Two independent transgenic lines were produced. Animal care was in compliance with regulations in Italy (D.M. 116192), Europe (O.J. of E.C.L. 358/1 12/18/c1986), and the United States (Animal Welfare Assurance No. A5594-01, Department of Health and Human Services, Washington, DC).

SCI

SCI was induced, as previously described [26]. Briefly, mice were anesthetized using chloral hydrate (400 mg/kg body weight). A longitudinal incision was made on the midline of the back, exposing the paravertebral muscles. These muscles were dissected away exposing T5-T8 vertebrae. The spinal cord was exposed via a 4-level T5-T8 laminectomy, and SCI was produced by extradural compression at T6-T7 level using an aneurysm clip with a closing force of 24 g. In all injured groups, the spinal cord was compressed for 1 minute. Sham animals were only subjected to laminectomy. Following surgery, 1.0 cc of saline was administered subcutaneously to replace the blood volume lost during the surgery. During recovery from anesthesia, the mice were placed on a warm heating pad and covered with a warm towel. The mice were individually housed in a temperature-controlled room at 27°C for a survival period of 10 days. Food and water were provided to the mice ad libitum. During this time period, the animals' bladders were manually voided twice a day until the mice were able to regain normal bladder function.

Experimental Groups

Mice were randomly allocated into the following groups: 1) SCI WT group, mice were subjected to SCI; 2) SCI $GILZ^{TG}$ group: mice were subjected to SCI; 3) control WT group (sham): WT mice were subjected to the surgical procedures, as with the previous groups, except that the aneurysm clip was not applied; and 4) control $GILZ^{TG}$ group (sham): $GITR^{TG}$ mice were subjected to the surgical

procedures, as with the previous groups, except that the aneurysm clip was not applied. In each experiment, we used 5 animals per group, unless otherwise indicated. Mice from each group were sacrificed at 24 h after SCI to collect samples for the evaluation of the parameters described as follows.

Myeloperoxidase Activity

Myeloperoxidase (MPO) activity, an indicator of polymorphonuclear leukocyte accumulation, was determined in the spinal cord tissues, as previously described [26] at 24 h after SCI. At the specified time, following SCI, spinal cord tissues were obtained and weighed, and each piece was homogenized in a solution containing 0.5% (w/v) hexadecyltrimethyl-ammonium bromide dissolved in 10 mM potassium phosphate buffer (pH 7) and centrifuged for 30 minutes at 20,000 × g at 4°C. An aliquot of the supernatant was then allowed to react with a solution of 1.6 mM tetramethylbenzidine and 0.1 mM H_2O_2. The rate of change in absorbance was measured spectrophotometrically at 650 nm. MPO activity was defined as the quantity of enzyme degrading 1 μmol of peroxide per minute at 37°C, and it was expressed as units of MPO/mg protein.

Preparation of Cytosolic and Nuclear Extracts from Spinal Cord and Western Blot Analysis

Cytosolic and nuclear extracts were prepared as previously described [27], with slight modifications. Briefly, tissue segments containing the lesion (1 cm on each side of the lesion) from each mouse were suspended in extraction buffer A containing 0.2 mM phenylmethylsulfonyl fluoride (PMSF), 0.15 mM pepstatin A, 20 mM leupeptin, 1 mM sodium orthovanadate, homogenized at the highest setting for 2 minutes, and centrifuged at 1,000 × g for 10 minutes at 4°C. Supernatants represented the cytosolic fraction. The pellets (containing enriched nuclei) were re-suspended in buffer B containing 1% Triton X-100, 150 mM NaCl, 10 mM tris-HCl pH 7.4, 1 mM ethylene glycol tetraacetric acid (EGTA), 1 mM ethylenediaminetetraacetric acid (EDTA), 0.2 mM PMSF, 20 μm leupeptin, 0.2 mM sodium orthovanadate. After centrifugation 30 minutes at 15,000 × g at 4°C, the supernatants containing the nuclear protein were stored at −80°C for further analysis. The levels of inhabitor of kappaB-α (IκB-α), glial fibrillary acidic protein (GFAP), Bax, and Bcl-2 were quantified in cytosolic fraction from spinal cord tissue collected after 24 h after SCI, whereas NF-κB p65 levels were quantified in nuclear fraction. Protein (40 μg) was dissolved in Laemmli Sample Buffer, boiled for 5 minutes, and subjected to sodium dodecyl Sulphate - polyAcrylamide gel electrophoresis (SDS PAGE) (8% or 15% polyacrylamide). The Western blot was performed by transferring proteins from a slab gel to nitrocellulose membrane at 240 mA for 40 minutes at room temperature using Trans-Blot SD Semi-Dry Transfer Cell (Bio-Rad, Milan, Italy). The filters were blocked with 1× phosphate buffered saline (PBS), 5 % (w/v) nonfat dried milk PBS and 5% mild (PM) for 40 minutes at room temperature and subsequently probed with specific Abs anti-IκB-α (1:1,000; Santa Cruz Biotechnology, Santa Cruz, CA, USA), or anti-Bax (1:500; Santa Cruz Biotechnology), or anti-Bcl-2 (1:500; Santa Cruz Biotechnology), or anti-GFAP (1:500; Santa Cruz Biotechnology), or anti-NF-κB p65 (1:1,000; Santa Cruz Biotechnology) in 1× PBS, 5% w/v nonfat dried milk, and 0.1% Tween-20 (PMT) at 4°C overnight. Membranes were incubated with peroxidase-conjugated bovine anti-mouse immunoglobulin G (IgG) secondary antibody or peroxidase-conjugated goat anti-rabbit IgG (1:2,000, Jackson ImmunoResearch, West Grove, PA) for 1 h at room temperature.

To ascertain that Western blots were loaded with equal amounts of protein lysates, they were also incubated in the presence of the antibody against β-actin (for cytosolic extract) or lamin A/C (for nuclear extract) proteins (1:10,000; Sigma-Aldrich Co., Milan, Italy).

Signals were detected with the enhanced chemiluminescence detection system reagent, according to manufacturer's instructions (SuperSignal West Pico Chemiluminescent Substrate, Pierce, Thermo Fisher Scientific Inc., Rockford, IL, USA). The relative expression of the protein bands of IκB-α (~37 kDa), GFAP (~50 kDa), NF-κB p65 (65 kDa), Bax (~23 kDa), and Bcl-2 (~26 kDa) were quantified by densitometry with ImageQuant TL software (GE Healthcare, Milan, Italy) and standardized for densitometric analysis to housekeeping gene levels. Images of Western blot signals were imported to analysis software (ImageQuant TL, v. 2003). A preparation of commercially available molecular weight markers (Precision Plus Protein Kaleidoscope standards, Bio-Rad) consisting of proteins of molecular weight 10 to 250 kDa, which was used to define molecular weight positions and as reference concentrations for each molecular weight.

Immunohistochemical Localization of Nitrotyrosine, iNOS, Bax and Bcl-2, CD4, CD8, Fas ligand, Tumor Necrosis Factor-α, Interleukin-2Rα, and Interleukin-1β

At the 24 h after SCI induction, the tissues were fixed in 10% (w/v) PBS-buffered formaldehyde, and 8-μm sections were prepared from paraffin-embedded tissues. After deparaffinization, endogenous peroxidase was quenched with 0.3% (v/v) hydrogen peroxide in 60% (v/v) methanol for 30 minutes. The sections were permeabilized with 0.1% (w/v) Triton X-100 in PBS for 20 minutes. Nonspecific

adsorption was minimized by incubating the section in 2% (v/v) normal goat serum in PBS for 20 minutes. Endogenous biotin or avidin binding sites were blocked by sequential incubation for 15 minutes with biotin and avidin (Vector Laboratories, Burlingame, CA, USA), respectively. Sections were incubated overnight with anti-nitrotyrosine rabbit polyclonal antibody (1:500 in PBS, v/v), with anti-iNOS polyclonal antibody rat (1:500 in PBS, v/v), anti-Bax rabbit polyclonal antibody (1:500 in PBS, v/v), or with anti-Bcl-2 polyclonal antibody rat, anti-CD4 rabbit polyclonal antibody (1:500 in PBS, v/v), anti-CD8α rabbit polyclonal antibody (1:500 in PBS, v/v), anti-Fas ligand (FasL) rabbit polyclonal antibody (1:500 in PBS, v/v), anti-TNFα rabbit polyclonal antibody (1:500 in PBS, v/v), anti-IL-2Rα rabbit polyclonal antibody (1:500 in PBS, v/v), and anti-IL-1β rabbit polyclonal antibody (1:500 in PBS, v/v). Sections were washed with PBS and incubated with a secondary antibody. Specific labeling was detected with a biotin-conjugated goat anti-rabbit IgG and avidin-biotin peroxidase complex (Vector Laboratories, Burlingame, CA, USA). To verify the binding specificity for nitrotyrosine, iNOS, Bax, and Bcl-2, CD4, CD8α, FasL, tumor necrosis factor (TNF)-α, interleukin (IL)-2Rα, and interleukin-1β, some sections were also incubated with only the primary antibody (no secondary) or with only the secondary antibody (no primary). In these situations, no positive staining was found in the sections indicating that the immunoreaction was positive in all the experiments carried out. Immunohistochemical photographs (n=5 photos from each sample collected from each mice in each experimental group) were assessed by densitometry, as previously described [28] by using Optilab Graftek software on a Macintosh personal computer, Optilab Graftek, Austin, TX; Macintoch personal computer (CPU G3-266).

Assessment of Apoptosis

Detection of cells with DNA strand breaks was performed in paraffin-embedded spinal cord section by the terminal deoxynucleotidyl transferase dUTP nick end labeling (TUNEL) technique using an Apop Tag-peroxidase kit (ApopTag® Peroxidase, Millipore, Billerica, MA, USA), as previously described [20]. Briefly, sections were incubated with 15 μg/ml proteinase K for 15 minutes at room temperature and then washed with PBS. Endogenous peroxidase was inactivated by 3% H_2O_2 for 5 minutes at room temperature and was then washed with PBS. Sections were immersed in terminal deoxynucleotidyl transferase (TdT) buffer containing TdT and biotinylated 2'-Deoxyuridine, 5'-Triphosphate (dUTP) in TdT buffer, incubated in a humid atmosphere at 37°C for 90 minutes, and then washed with PBS. The sections were incubated at room temperature for 30 minutes with anti-horseradish peroxidase-conjugated antibody, and the signals were visualized with diaminobenzidine. Negative and positive controls were performed in every assay. As negative controls, tissue sections were processed in an identical manner, except that the terminal TdT enzyme was substituted with the same volume of PBS. In each tissue section, the number of positive cells was determined via stereological counting methods, which were counted in 20 optical fields in the area of 1.0-mm rostral and caudal to the epicenter (2-mm long total) following the scheme reported in Supplementary Figure 1.

Light Microscopy

Spinal cord tissues were taken at 24 h following trauma, and were fixed for 24 h in paraformaldehyde solution (4% in PBS 0.1 M) at room temperature, dehydrated by graded ethanol, and embedded in Paraplast (Sherwood Medical, Mahwah, NJ). Tissue sections (thickness, 5 μm) were deparaffinized with xylene, stained with hematoxylin & eosin, and studied using light microscopy (Dialux 22, Leitz, Germany). All the histological studies were performed in a blinded fashion. Segments of each spinal cord were evaluated by an experienced histopathologist. Damaged neurons were counted and the histopathologic changes of the gray matter were scored on a 6-point scale [26]: 0 = no lesion observed; 1 = gray matter contained 1 to 5 eosinophilic neurons; 2 = gray matter contained 5 to 10 eosinophilic neurons; 3 = gray matter contained more than 10 eosinophilic neurons; 4 = small infarction (less than one third of the gray matter area); 5 = moderate infarction; (one third to one half of the gray matter area); 6 = large infarction (more than one half of the gray matter area). The scores from all the sections from each spinal cord were averaged to give a final score for an individual mouse. All the histological studies were performed in a blinded fashion.

Enzyme-Linked Immunosorbent Assay Measurement of TNF-α, IL-1β, and IL-10

For the measurement of cytokines levels, a 1 cm sample containing the lesion site (or comparable region of sham-operated animals) was rapidly dissected and homogenized in 1 ml PBS containing protease inhibitors (Complete protease inhibitor tablets, Roche). TNF-α, IL-1β, and IL-10 levels were assayed using DuoSet ELISA Development System (R&D Systems, Minneapolis, MN, USA). All assays were carried out in duplicate using recommended buffers, diluents, and substrates. Absorbency was determined using a microplate reader at 450 nm (Multiskan FC Microplate Photometer, Thermo Fisher Scientific Inc., Rockford, IL, USA). The intra-assay coefficient of variations for both assays was less than 10%. The concentration of the cytokines in the tissue was mentioned as protein in pg/mg.

Determination of Prostaglandin E2 (PGE_2) in Mouse Spinal Cords

The spinal cords were collected at 24 h after SCI from the animals (2 to 6 spinal cords were pooled together) and immediately homogenized in methanol. The mediators in the tissues were extracted in 5 ml methanol for 3 to 5 days at −80°C. To remove the tissue residues, the extracts were centrifuged at 1,800 g for 20 minutes at 4°C. Then the sample solutions were dried to remove methanol. The dried samples were suspended in an assay buffer that was supplied with each ELISA kit (Assay Designs, Ann Arbor, MI, USA). To determine the levels of prostaglandin E2 (PGE_2) within the sensitive (i.e., linear) ranges of the standard curves, the samples were diluted further 1- to 20-fold and assayed at multiple dilutions [26].

Materials

Unless otherwise stated, all compounds were obtained from Sigma-Aldrich Company Ltd. (Milan, Italy). (All stock solutions were prepared in nonpyrogenic saline (0.9% NaCl; Baxter, Italy) or 10% dimethyl sulfoxide.

Statistical Evaluation

All values in the figures and the text are expressed as mean ± SEM. Results shown in the figures are representative of at least 3 experiments performed on different experimental days. In each experiment, we used 5 animals per group, unless otherwise indicated. The results were analyzed by one-way analysis of variance followed by a Bonferroni post-hoc test for multiple comparisons. A p value of less than 0.05 was considered significant.

Results

GILZ Over-Expression Reduces iNOS, Nitrotyrosine, and the Damage of the Spinal Cord Tissue

To evaluate the possible role of GILZ over-expression on degree of SCI induction, the severity of the trauma was measured at 24 h after injury (Fig. 1). Results show an increased damage of the spinal cord in tissue of WT mice subjected to SCI (Fig. 1C) as compared to $GILZ^{TG}$ with SCI (Fig. 1D). Notably, the extent and severity of the histological signs of SCI in $GILZ^{TG}$ mice (Fig. 1D) was significantly reduced as compared to WT (Fig. 1C), as also indicated by the histological score (Fig. 1E). The histological pattern of SCI previously described appeared to be correlated with cellular changes into the spinal cord. The cellular changes occurring in the perilesioned zone (namely, at the boundary between the core necrotic area and the penumbra zone) were evaluated by the expression of specific glial/precursor cell markers. In line with previous literature data [29], a significant increase in the expression of GFAP was found in the perilesioned area of WT mice subjected to SCI with respect to sham-operated animals (Fig. 1F). On the contrary, significant less GFAP expression was found in the spinal cord tissues after SCI collected from $GILZ^{TG}$ mice (Fig. 1F).

iNOS is known to catalyze the oxidation of the guanidine group of L-arginine to nitric oxide (NO), whereas nitrotyrosine indicates the site of peroxynitrite production and oxidative stress, providing evidence of the toxicity of NO in a number of diseases [30]. Thus, iNOS and nitrotyrosine over-expression account for NO production and the consequent neurodegenerative changes [31, 32]. Twenty-four hours after SCI induction, iNOS and nitrotyrosine were measured by immunohistochemical analysis in the spinal cord sections to determine the localization of peroxynitrite formation and/or other nitrogen derivatives produced during SCI. Sections of spinal cord from sham-operated mice did not stain for iNOS or nitrotyrosine (Fig. 1G, M, H, and N, respectively), whereas spinal cord sections obtained from WT mice with SCI exhibited positive staining for iNOS (Fig. 1I) and nitrotyrosine (Fig. 1O). The positive staining was mainly localized in infiltrating inflammatory cells, as well as in nuclei of Schwann cells. After SCI induction the staining for iNOS and nitrotyrosine were visibly and significantly reduced in $GILZ^{TG}$ (Fig. 1L and P, respectively) as compared to WT mice. These results indicate that GILZ over-expression in T lymphocytes inhibits SCI-induced iNOS and nitrotyrosine induction and neuronal tissue damage.

Effect of GILZ Over-Expression on IκB-α Degradation and NF-κBp65 Nuclear Translocation

NF-κB has an important role in T-cell activation and in inflammation. To analyze the molecular mechanisms responsible for GILZ anti-inflammatory activity, we evaluated the classical NF-κB pathway [33, 34] measured by Western blot IκB-α levels and nuclear translocation of NF-κB (NF-κB p65) twenty-four hours after SCI induction. A basal level of IκB-α was detected in the spinal cord from both WT and $GILZ^{TG}$ sham-operated animals (Fig. 2A); SCI substantially reduced IκB-α levels in WT mice. SCI-induced IκB-α reduction was significantly inhibited in $GILZ^{TG}$ mice (Fig. 2A) as also indicated by densitometric analysis (Fig. 2A1).

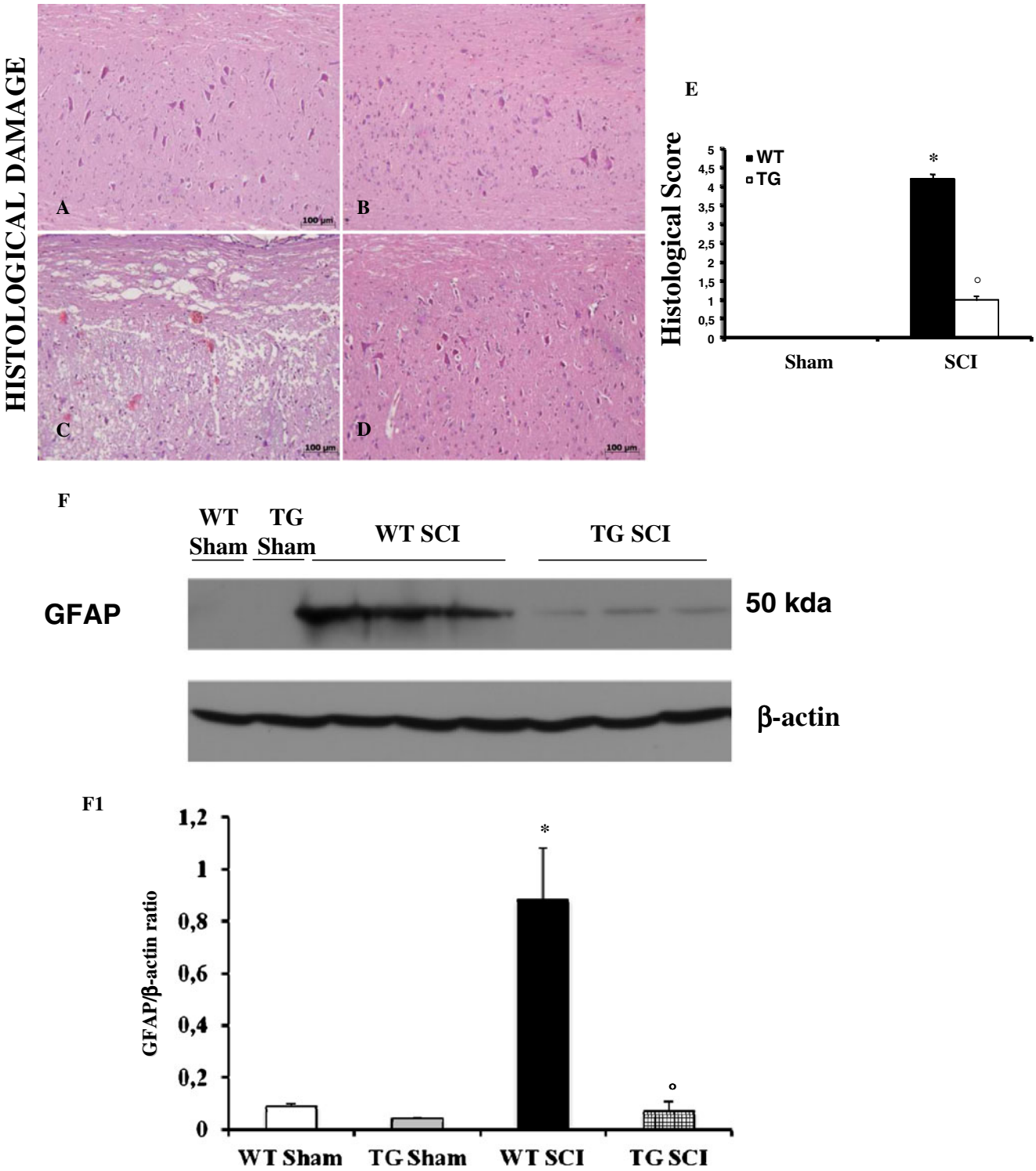

In addition, we readily detected an increase of nuclear translocation of p65, the main transactivating NF-κB subunit in WT spinal cord 24 hours after trauma (Fig. 2B, B1). GILZ over-expression in $GILZ^{TG}$ significantly decreased the nuclear content of NF-κB p65 (Fig. 2B, B1). These results indicate that GILZ over-expression counters NF-κB activation in SCI.

GILZ Over-Expression Inhibits the SCI-Induced Increase of MPO, TNF-α, IL-1β, and IL-10

MPO activity is a measure of inflammatory cells migration into the tissue. MPO levels were increased in WT, at 24 h after SCI induction, as compared with tissues obtained from sham-operated animals. A significantly decreased MPO

◀ **Fig. 1** Effect of GILZ on histological alterations of the spinal cord tissue and immunohistochemical localization of iNOS and nitrotyrosine. No histological alteration was observed in the spinal cord tissues from sham-operated mice (A,B). Twenty-four h after SCI a significant damage was evident in spinal cord from WT mice, as also indicated by the presence of edema as well as alteration of the white matter (C). Notably, a significant protection from the SCI was observed in the tissue from $GILZ^{TG}$ mice (D). The histological scoring of injury severity showed that the degree of injury is higher in mice SCI-operated mice, when compared with SCI $GILZ^{TG}$ mice and sham-operated mice (E). Moreover, the cellular changes occurring in the perilesioned zone (namely, at the boundary between the core necrotic area and the penumbra zone) were evaluated by the expression of GFAP, a specific glial/precursor cell markers. The increased levels of GFAP protein were significantly reduced in the spinal cord tissues from $GILZ^{TG}$ as compared to WT mice (F,F1). Immunoblottings in panel F is representative of one spinal cord out of 5 analyzed. The densitometry results in panel F1 are expressed as mean±s.e.m. of 3 blots. Histological score data are expressed as mean ± s.e.m. of 6 mice each group. *$p<0.01$ *vs.* sham; °$p<0.01$ *vs.* SCI-operated mice. GILZ over-expression in SCI operated mice produced a marked reduction in the immunostaining for iNOS (L) and nitrotyrosine (P) in spinal cord tissue, when compared to positive iNOS (I) and nitrotyrosine (O) staining obtained from the spinal cord tissue from WT mice 24 h after the injury. No positive staining was detected in sham-operated mice for iNOS or nitrotyrosine (G, H and M,N respectively). This figure is representative of 3 experiments performed on different experimental days

activity was observed in tissue taken from $GILZ^{TG}$, as compared to WT mice (Fig. 3A).

Tissue IL-10 levels in injured WT mice were significantly elevated. $GILZ^{TG}$ mice had significantly higher tissue IL-10 levels than WT mice. At 24 h after SCI, increased levels of TNF-α (Fig. 3C) and IL-1β (Fig. 3D), as evaluated by ELISA, were observed in spinal cord tissue extracts from WT animals. In $GILZ^{TG}$ mice, production of TNF-α (Fig. 3C) and IL-1β (Fig. 3D) was significantly reduced. Low expression of TNF-α (Fig. 3C) and IL-1β (Fig. 3D) was detected in sham-operated mice.

Moreover, the levels of PGE_2 in spinal cord were markedly elevated in injured WT mice, as compared to $GILZ^{TG}$ mice (Fig. 4).

In addition, tissue sections obtained from SCI in WT animals showed positive staining for TNF-α (Fig. 5C) and IL-1β (Fig. 5G), whereas in $GILZ^{TG}$ mice the staining for TNF-α (Fig. 5D) and IL-1β (Fig. 5H) was visibly and significantly reduced. In the spinal cord tissue sections of sham animals, no positive staining was observed for TNF-α (Fig. 5A, B) or IL-1β (Fig. 5E, F).

Activated T cells over-express a number of membrane molecules, including IL-2Rα. Therefore, we examined the expression of IL-2Rα subunits in spinal cord tissue sections. Immunohistological staining for IL-2Rα in the spinal cord was determined 24 h after SCI induction. Spinal cord sections from sham-operated mice (both WT and $GILZ^{TG}$) did not stain for IL-2Rα (Fig. 5I, L), whereas spinal cord sections obtained from WT mice exhibited positive staining for IL-2Rα (Fig. 5M). GILZ over-expression in $GILZ^{TG}$ mice reduced the degree of positive staining for IL-2Rα (Fig. 5N).

These results demonstrate that GILZ over-expression reduces T-lymphocyte activation, cell infiltration in spinal cord tissue, and production of proinflammatory cytokines.

Effects of GILZ on Apoptosis in the Injured Spinal Cord

To test whether spinal cord damage was associated to apoptosis, we measured TUNEL-like staining in the perilesional spinal cord tissue. Almost no apoptotic cells were detected in the spinal cord from sham-operated mice (Fig. 6A, B). At 24 h after the trauma induction, tissues from SCI in WT mice demonstrated a marked appearance of dark brown apoptotic cells and intercellular apoptotic fragments (Fig. 6C, see particle C_1). In contrast, tissues obtained from $GILZ^{TG}$ mice (Fig. 6D) demonstrated a reduced number of apoptotic cells or fragments.

As Bax and Bcl-2 are important apoptosis regulators, at 24 h after SCI we investigated the changes in Bax and Bcl-2 expression in spinal cord homogenates by Western blot. Bax levels were appreciably increased in the spinal cord from WT mice subjected to SCI as compared to sham. A significant reduction was evident in injured $GILZ^{TG}$ mice (Fig. 7A, see also densitometry analysis A1). Furthermore, we also analyzed Bcl-2 expression. A basal level of Bcl-2 expression was detected in spinal cord from sham-operated mice (Fig. 7B, see densitometry analysis B1). Twenty-four hours after SCI, the Bcl-2 expression was significantly reduced in spinal cord from WT mice with SCI (Fig. 7B, see densitometry analysis B1). GILZ over-expression in $GILZ^{TG}$ mice significantly countered the SCI-induced inhibition of Bcl-2 expression (Fig. 7B, see densitometry analysis B1).

Moreover, samples of spinal cord tissue were taken at 24 h after SCI to determine levels of Bax and Bcl-2 expression by immunohistological staining. Sections of spinal cord from sham-operated mice did not stain for Bax (Fig. 7C, D), whereas spinal cord sections obtained from WT mice with SCI exhibited a positive staining for Bax (Fig. 7E). GILZ over-expression in $GILZ^{TG}$ mice reduced the degree of positive staining for Bax in the spinal cord of mice subjected to SCI (Fig. 7F). In addition, spinal cord sections from sham-operated mice demonstrated Bcl-2 positive staining (Fig. 7G, H), whereas the staining was significantly reduced after SCI induction in the WT mice (Fig. 7I). The loss of positive staining for Bcl-2 was attenuated in $GILZ^{TG}$ mice (Fig. 7L). These results indicate GILZ over-expression in T lymphocytes inhibits neural cell apoptosis.

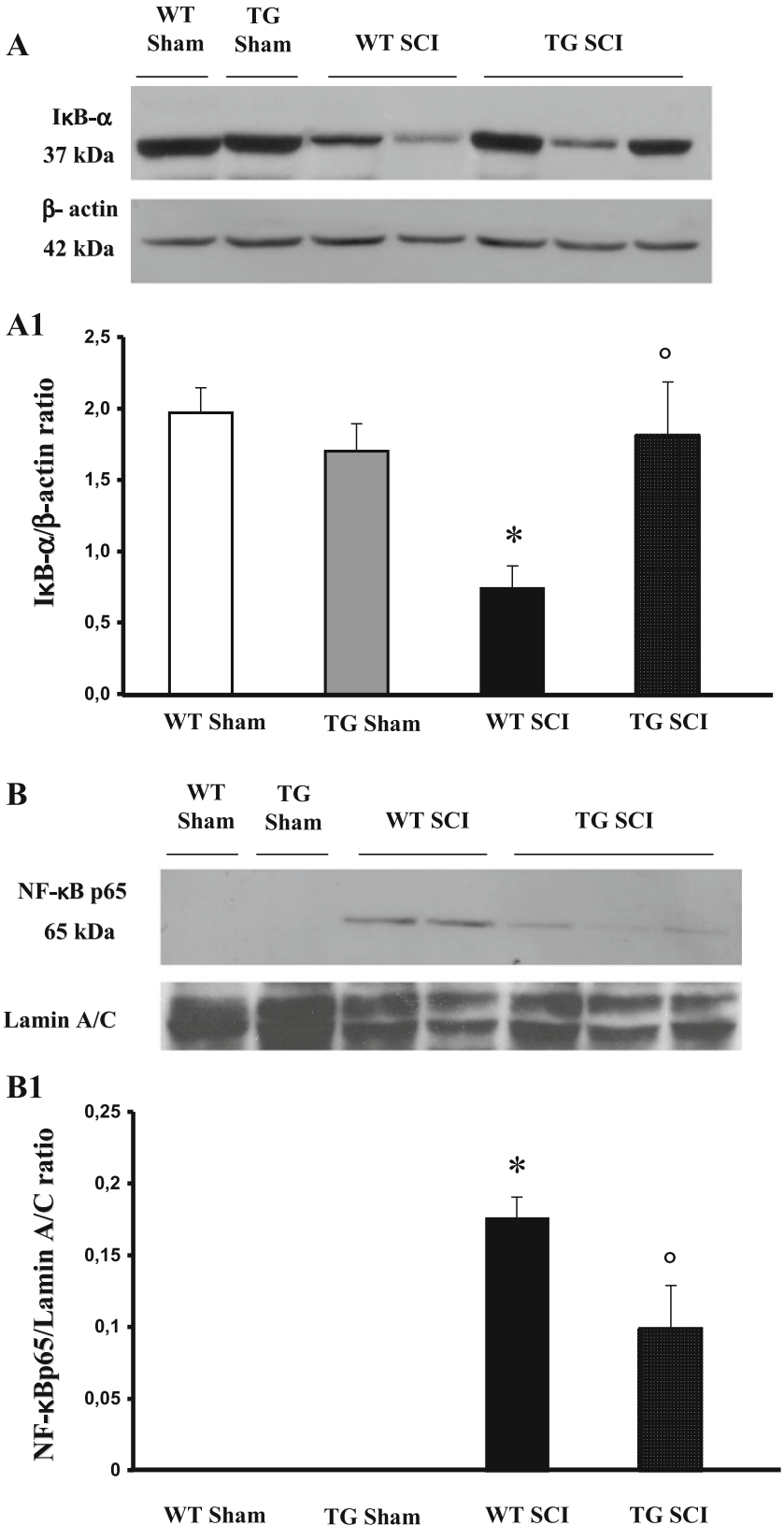

Fig. 2 Effect of GILZ over-expression on IκB-a degradation and NF-κB p65 nuclear translocation. A basal level of IκB-a was detected in the spinal cord from sham-operated animals (A, A1) that was substantially reduced 24 h after SCI induction in WT mice (A, A1). GILZ over-expression, in $GILZ^{TG}$ mice, prevented the SCI-induced IκB-a reduction (A, A1). In addition, the levels of NF-κB p65 protein were significantly reduced in the nuclear fractions of the spinal cord tissues animals from $GILZ^{TG}$ as compared to WT mice (B,B1). Immunoblottings in panel A and B are representative of one spinal cord out of 5 analyzed. The densitometry results in panel A1 and B1 were obtained by phosphoimager analysis and are expressed as mean±s.e.m. of 2 blots *$p<0.05$ versus sham, °$p<0.05$ versus SCI-operated mice

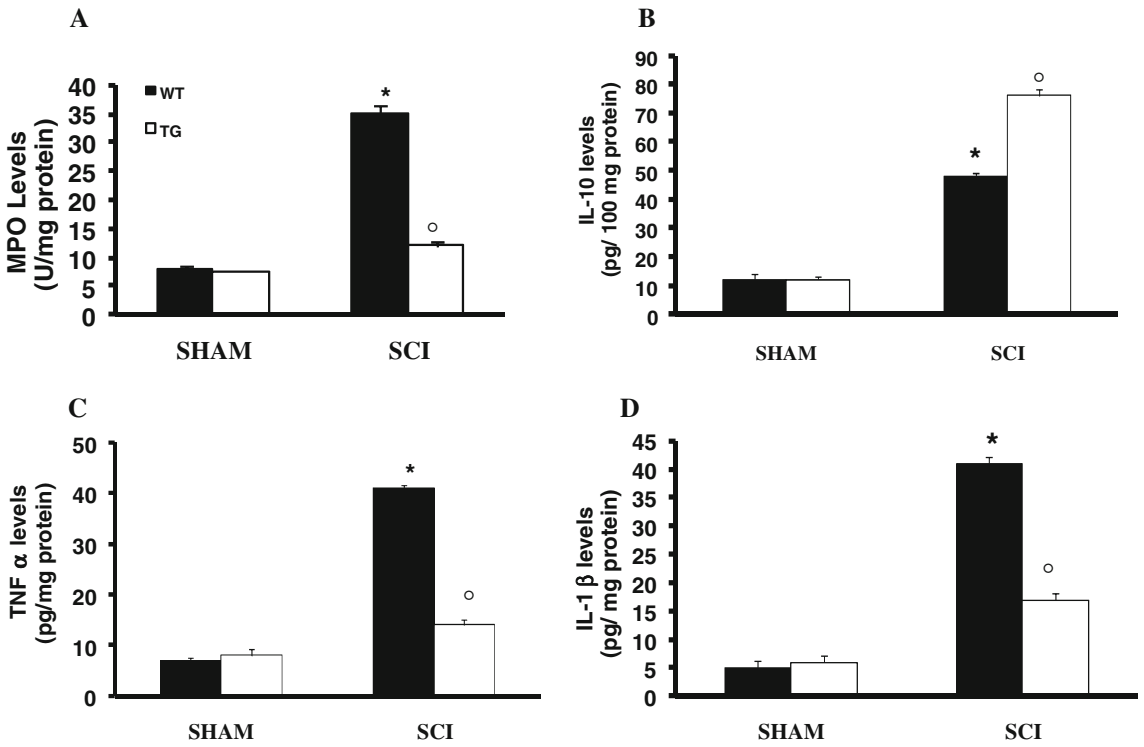

Fig. 3 Effect of GILZ over-expression on MPO activity, production of TNF-a, IL-1b, and IL-10. Myeloperoxidase (MPO) levels were increased by spinal cord injury in WT mice as compared with tissues obtained from sham animals. In contrast, a decrease MPO activity was observed in tissue taken from $GILZ^{TG}$ mice 24 h after injury (A). The evaluation of the production of inflammatory cytokines IL-10, TNF-a and IL-1b, by ELISA, showed that in spinal cord samples, taken after 24 h after injury, there was a substantial increase in IL-10 (B), TNF-a (C) and IL-1b (D) formation when compared with sham-operated animals. In contrast, in $GILZ^{TG}$ mice there were a significant increase of IL-10 (B), and inhibition of TNF-a (C) and IL-1b (D) as compared to WT. Data are mean±s.e.m. of 6 mice for each group. *$p<0.01$ *vs* sham, °$p<0.01$ vs SCI-operated mice

Effect of GILZ Over-Expression on FasL Expression, CD8α+, and CD4+ T Cells Infiltration after SCI

FasL expression is up-regulated during inflammation in many cells, including activated T lymphocytes. Moreover, we evaluated FasL expression at 24 h after SCI induction, as it has been reported that apoptosis triggered by Fas-Fas ligand binding plays a fundamental role in the regulation of the immune system. Spinal cord sections from sham-operated mice did not stain for FasL (Fig. 8A, B), whereas spinal cord sections from WT with SCI mice exhibited positive staining for FasL (Fig. 8C), mainly localized in infiltrating inflammatory cells and in the nuclei of Schwann cells. Consistent with apoptosis inhibition, $GILZ^{TG}$ mice showed a reduced FasL staining (Fig. 8D).

Reduction of FasL positive (FasL+) cells is consistent with inhibition of inflammation and tissue damage. This could be related to decreased tissue infiltration of activated T lymphocytes. In fact, it has been shown that in the early time of inflammation T lymphocytes infiltrated into the inflammatory area [35]. The infiltrating lymphocyte population was further characterized to determine the contributions by T-cell subsets. Spinal cords obtained from WT mice, 24 h after SCI induction, showed an increased infiltration of CD8α + (Fig. 8G) and of CD4+ (Fig. 8M, M1) T cells when compared with sham-operated animals

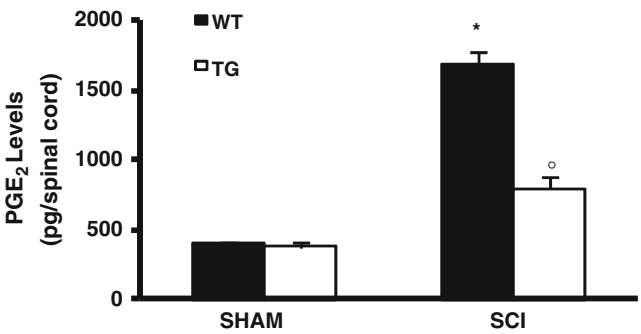

Fig. 4 Effect of GILZ over-expression on PGE2 levels PGE2 levels were increased by SCI in WT mice as compared with tissues obtained from sham animals. Mice with GILZ over-expression showed a reduction of PGE2 levels

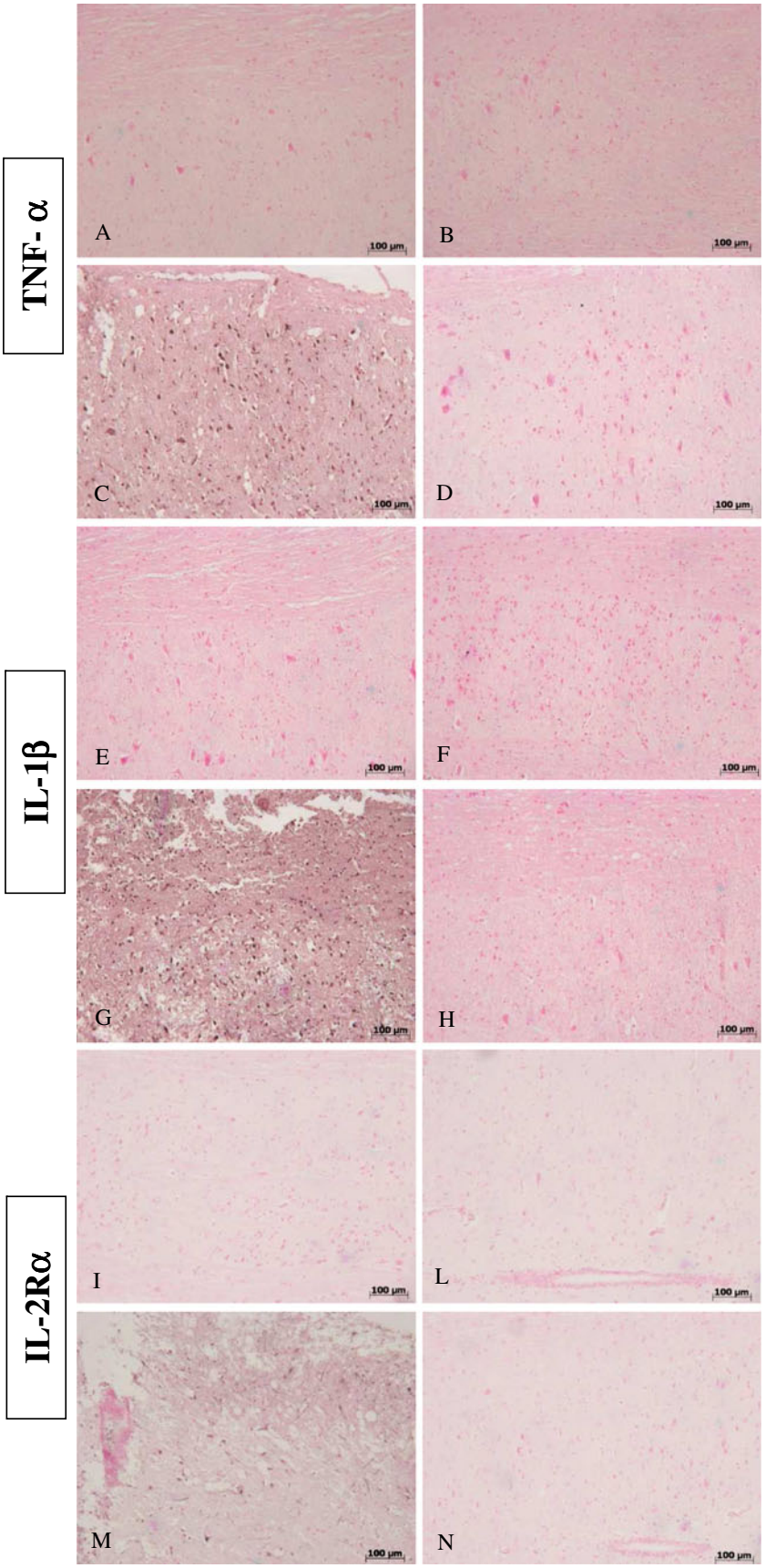

Fig. 5 Effects of GILZ on tissue expression of TNF-a, IL-1b and IL-2Ra, after SCI, as evaluated by immuno-histochemistry Positive staining for TNF-a (C) and IL-1b (G) was observed in spinal cord tissue sections obtained from SCI GILZ^{WT} animals. The staining for TNF-a (D) and IL-1b (H) in SCI GILZ^{TG} mice was reduced significantly in the tissues collected at 24 h. Spinal cord sections from sham-operated mice not shown stain for TNF-a (A,B) and IL-1b (E,F) Moreover, spinal cord sections from sham-operated mice did not stain for IL-2Ra (I and L). Spinal cord sections obtained from WT mice exhibited positive staining for IL-2Ra (M) after SCI induction. GILZ overexpression in GILZ^{TG} mice reduced the degree of positive staining for IL-2Ra in the spinal cord (N)

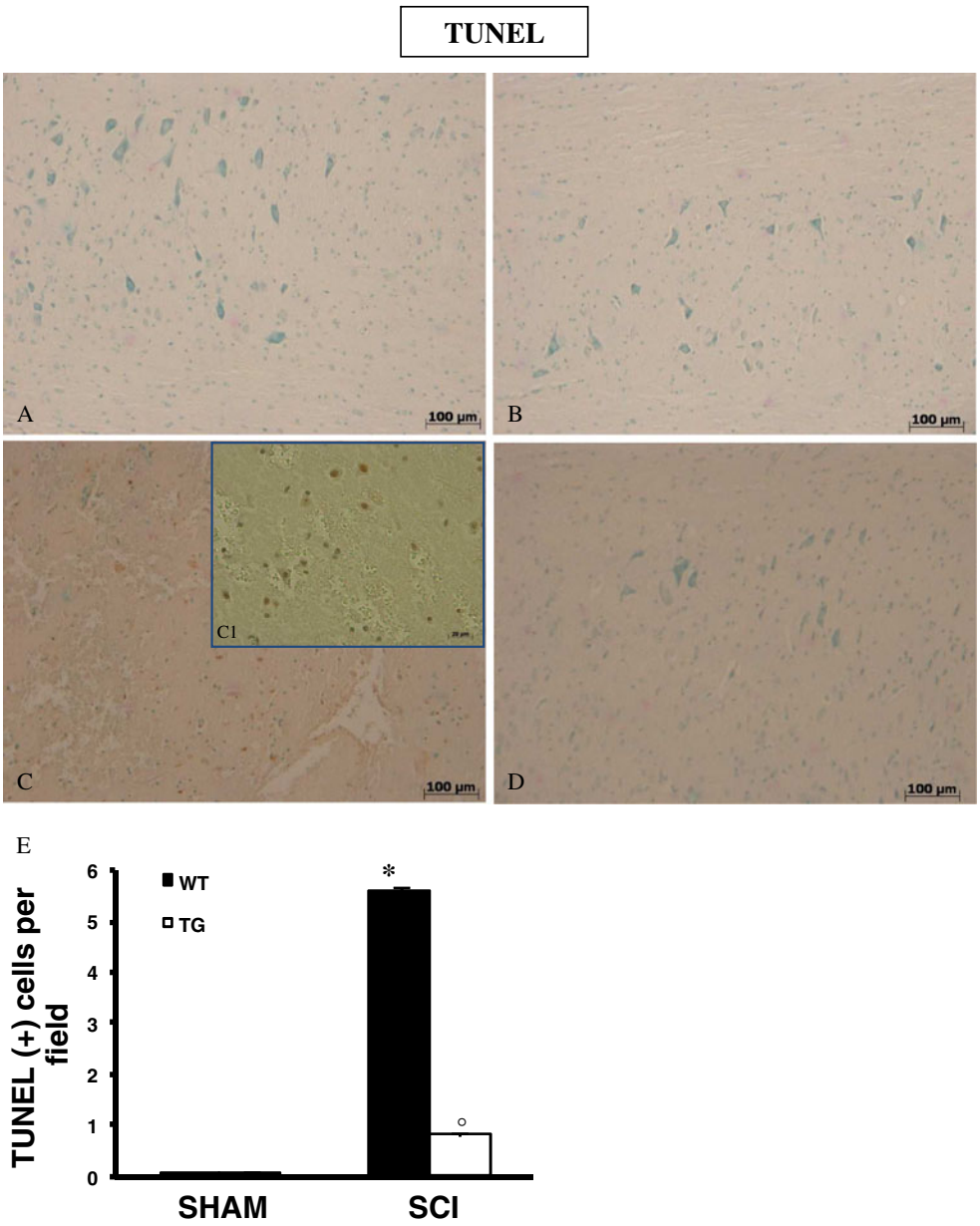

Fig. 6 Effects of GILZ on apoptosis as evaluated by TUNEL coloration in spinal cord tissue sections. The number of apoptotic fragments and cells increased at 24 h after SCI induction (C), associated with a specific apoptotic morphology characterized by the compaction of chromatin into uniformly dense masses in perinuclear membrane, the formation of apoptotic bodies as well as the membrane blebbing (see particle C1). In contrast, tissues obtained from $GILZ^{TG}$ mice (D) demonstrated a small number of apoptotic cells or fragments. No staining was found in shamoperated mice (A-B). In SHAM-operated animals, the central area of each tissue section was taken as a reference point and an identical number of optical fields was counted (see Supplementary Figure 1 for details). Data are reported as mean± standard error. For each staining, at least 20 optical fields from sections taken from 3 different animals were counted. *$p<0.01$ *vs.* sham; °$p<0.01$ *vs.* SCI-operated mice

(Fig. 8E, F and I, L, respectively). GILZ over-expression in $GILZ^{TG}$ mice reduced the degree of staining for CD8α + (Fig. 8H) and CD4+ (Fig. 8N) cells.

These results indicate that selective GILZ over-expression in T lymphocytes significantly reduces the number of infiltrating CD8α + and CD4+ T lymphocytes.

Discussion

The results presented here clearly indicate that levels of inflammation and tissue damage in a mouse SCI model are significantly lower in $GILZ^{TG}$ mice, in which GILZ is selectively over-expressed in T lymphocytes than in WT littermates. Moreover, we show that GILZ over-expression inhibits SCI-induced NF-κB activation and nuclear translocation, as well as T cell migration, into the inflammatory tissue.

Inflammation is a well-regulated physiological process aimed to maintain the homeostatic control of tissues and organs integrity. A number of cellular and molecular events, such as those responsible for cell activation and production of soluble factors, are responsible for this complex process. In particular, activated T lymphocytes have been described to be involved in the inflammatory process development and maintenance.

SCI usually begins with a traumatic blow of the spine followed by various pathological changes in neural tissue, such as reduced activity and survival of neurons. The primary tissue damage is followed by infiltration of immune cells, including T

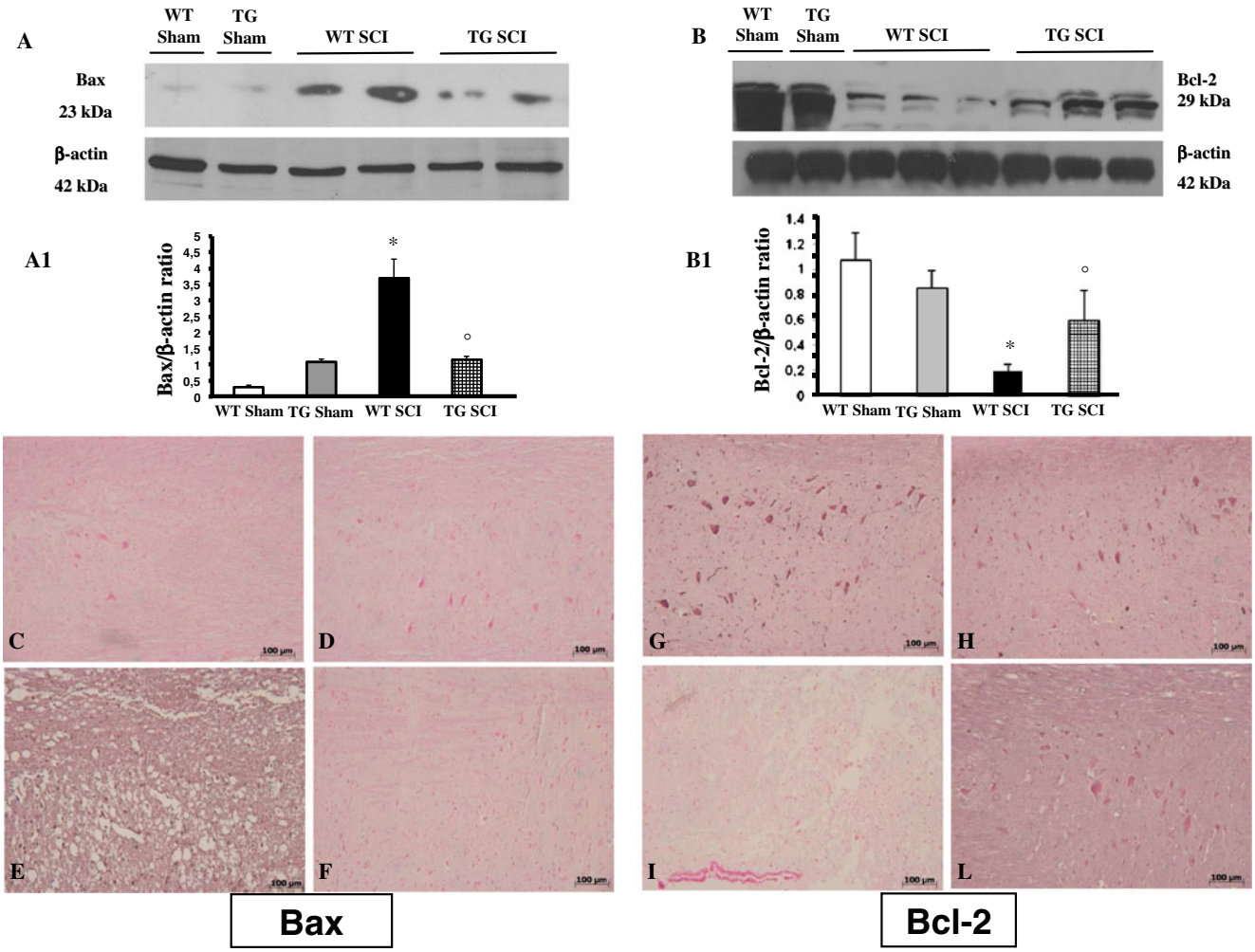

Fig. 7 Effects of GILZ on Bax and Bcl-2 levels, as evaluated by western blot and by immunohistochemical staining. Western blot analysis was realized in spinal cord tissue collected at 24 h after injury. (A) Sham: basal level of Bax was present in the tissue from-sham-operated mice. SCI WT: Bax band is more evident in the tissue from spinal cord injured mice. SCI GILZ^{TG}: Bax band is reduced in the tissue from spinal cord injured mice. (B) Sham: basal level of Bcl-2 was present in the tissue from-sham-operated mice. SCI WT: Bcl-2 band is reduced in the tissue from spinal cord injured mice. SCI GILZ^{TG}: Bcl-2 band is more evident in the tissue from spinal cord injured mice. Immunoblottings in panel A and B are representative of one spinal cord tissues out of 3 analyzed. The results in panel A1 and B1 (densitometry measured by Phosphoimage analysis, GE Healthcare, Milan, Italy) are expressed as mean±s.e.m.. *$p<0.01$ *vs.* Sham; °$p<0.01$ *vs.* SCI GILZ^{WT}. No positive staining for Bax was observed in the tissue section from sham-operated mice (C,D). SCI caused, at 24 h, an increase in the release of Bax expression (E). GILZ over-expression significantly inhibited the SCI-induced increase in Bax expression (F). On the contrary positive staining for Bcl-2 was observed in the spinal cord tissues of sham-operated mice (G,H). At 24h after SCI significantly less staining for Bcl-2 was observed (I). GILZ over-expression significantly prevented the loss of Bcl-2 expression induced by SCI (L). Figure is representative of at least 3 experiments performed on different experimental days

lymphocytes, and the release of proinflammatory mediators that cause a secondary and extended inflammation with tissue degeneration [35, 36]. The current therapeutic approach for SCI is limited to MP administration. The neuroproctective effects of MP has been proposed on the basis of inhibition of reactive nitrogen species peroxynitrite and its highly reactive free radicals [10, 11]. The potent anti-inflammatory activity of MP suggest that neuroprotective effects and improvement of motor recovery in human SCI after of high-dose MP treatment is also due to its immunosuppressive properties [11, 12]. However, although clinical results are promising, there is a growing concern that the therapeutic MP treatment is not worth of the associated risk of infection, pneumonia and septic shock, diabetic complications, gastrointestinal bleeding, and delayed wound healing. Therefore, as the case of other inflammatory and autoimmune diseases is important to monitor the efficacy of treatment and to develop new pharmacological approaches for therapy of SCI, our present study indicates a role of GILZ in controlling SCI-induced inflammation. In particular, using transgenic mice, in which

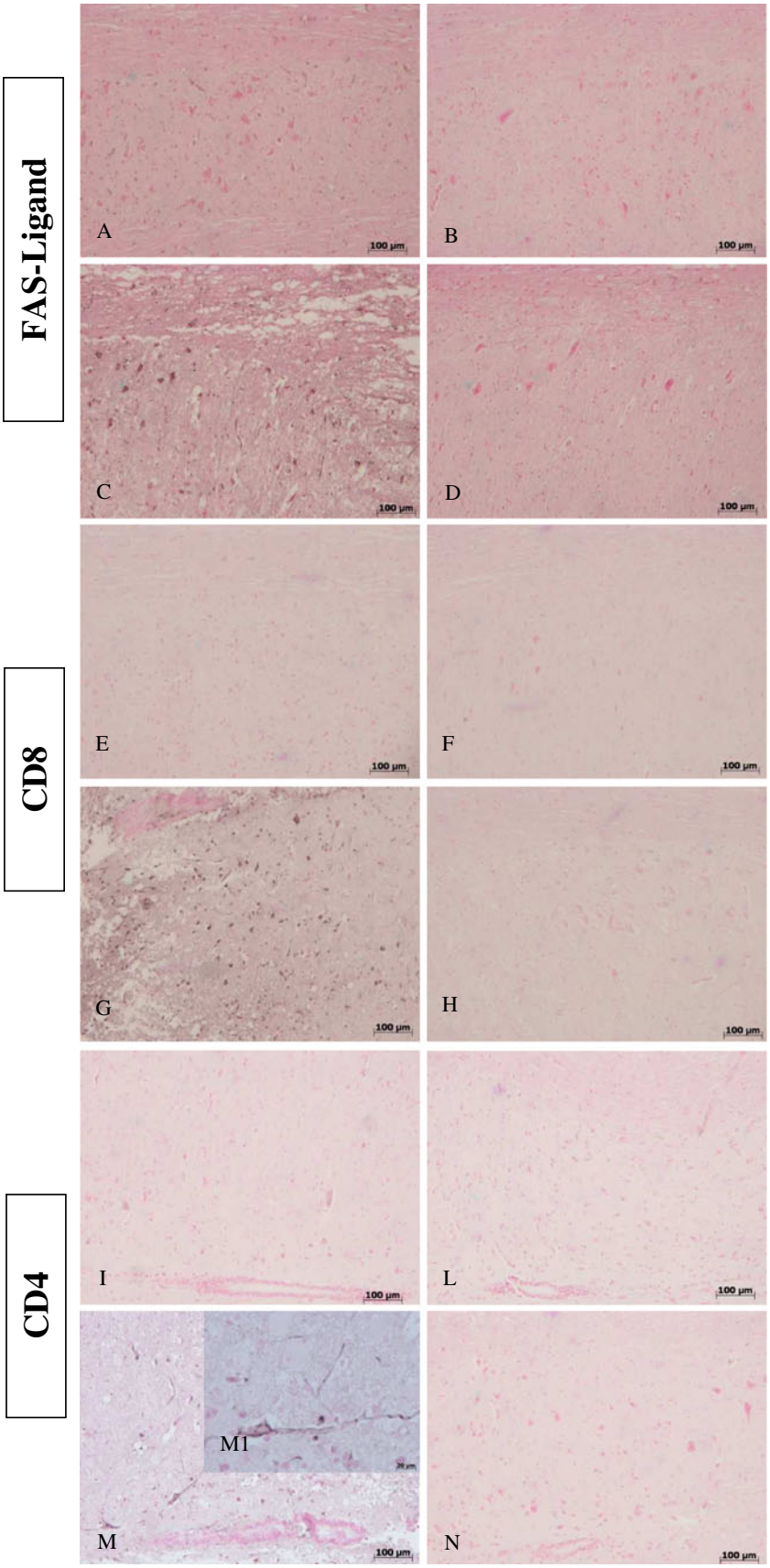

Fig. 8 Effects of GILZ on expression of FasL, CD4+ and CD8a+ T cells, after SCI. Immunohistological staining for FasL in the spinal cord was also determined 24 h after injury. No positive staining for sham-operated mice (A, B). Spinal cord sections obtained from SCI WT mice exhibited positive staining (C) mainly localized in inflammatory cells as well as in nuclei of Schwann cells. Inhibition of expression of GILZ reduced the degree of positive staining for FasL in the spinal cord (D). Spinal cords obtained from SCI WT mice showed significant accumulation of CD8a+ (G) and CD4+ (M, particle M1) T cells, when compared with sham operated animals (E,F and I,L, respectively). GILZ over-expression reduced the degree of positive staining for CD8a+ (H) and CD4+ (N) T cells in the spinal cord.

GILZ is selectively over-expressed in T lymphocytes at levels comparable to that obtained with dexamethasone treatment [20, 24, 25], we demonstrate that T lymphocytes play an important role in SCI.

To react against an antigen and engage tissue inflammation, activated T lymphocytes must leave the bloodstream and enter into the tissue. This is an important mechanism because it has been shown that in the early stages of inflammation, activated T lymphocytes participate to constitute the cell population that infiltrates into the inflammatory area in SCI [6, 35]. Herein, we show that FasL + and CD25+ (two markers of T cells activation) T lymphocytes (both CD4+ and CD8α+) infiltrate the damaged tissue during SCI. However, GILZ over-expression significantly decreases their numbers further demonstrating that activated T lymphocytes are important in the disease and showing that GILZ inhibits the T lymphocyte capability to induce an inflammatory process *in vivo*. These results are in accordance with observations suggesting GILZ can inhibit T-lymphocyte activation, cytokine production, and the inflammatory processes *in vitro* and *in vivo* [15–18, 20, 24, 37, 38]. Moreover, results described herein are also in accordance with the GILZ capability to counter NF-κB activation [16, 17, 21, 39], and in fact a significant inhibition of SCI-induced NF-κB activation and nuclear translocation is evident in $GILZ^{TG}$ mice. Notably, this NF-κB inhibition may well explain the lower inflammation that develops in $GILZ^{TG}$, in comparison to WT mice, after SCI induction. This observation may be of interest because it has been described, in SCI, as a strain-dependent difference in T-cell infiltration and inflammation, as related to differences in endogenous GC production [7]. Herein, we show a role of GILZ (a GC mediator) in regulating T-cell migration and inflammation development into the spinal lesion.

It is known that neutrophils also infiltrate and participate in the inflammatory process, thus contributing to tissue degeneration. Degeneration begins 24 h after trauma and increases during the next few days, with death of oligodendrocytes and cyst formation within the gray matter and the white matter. The building of a scar (mainly constituted of astrocytes and fibroblasts) [3] represents the final stage of SCI evolution [40]. Clearly all these events are inhibited in $GILZ^{TG}$ mice as a consequence of the inhibition of T-cell activation and migration into the lesion, a prerequisite for the entry of neutrophils into the inflammatory tissue. Thus, GILZ-mediated inhibition of T-cell activity is enough to counter the inflammatory cell infiltration process in SCI.

Previously, it has been shown that between 12 h and 72 h after experimental SCI induction, gene expression of proinflammatory cytokines and their receptors, including IL-1β, TNF-α, and IL-10, is significantly increased [41–44]. This indicates the importance of the role of soluble factors in mediating the inflammatory process, including the recruitment of inflammatory cells into the injury site [45]. Moreover, the proinflammatory cytokines induce other biochemical signals leading to the degeneration of myelin and apoptosis of neurons that cause the neurological deficit [46, 47]. Herein, we show that inhibition of proinflammatory cytokines is detected in $GILZ^{TG}$, including the production of TNF-α and IL-1β, which are crucial factors for inflammation development [4, 7, 35]. These results correlate with the decrease in NF-κB activation and nuclear translocation, an event important for the production of cytokines, and with the reduction of T cells infiltrating the spinal cord of $GILZ^{TG}$ mice, as compared to WT.

Results from previous studies show an increased iNOS and peroxynitrite in the injured spinal cord [31]. Moreover, high PGE_2 concentrations reflecting an increased activity of cyclooxygenase (COX)-2 are observed in the injured spinal cord, and we show reduced levels of PGE_2 in the spinal cord from $GILZ^{TG}$ mice. In addition, it has been demonstrated that consequent to cell infiltration and cytokine production, NO is produced and accounts (at least in part) for the neurodegenerative changes [32]. In fact, NO production can contribute to cell death, tissue damage, and degeneration observed in SCI. iNOS and nitrotyrosine are reduced in $GILZ^{TG}$ mice, thus indicating for a diminished NO production, and this reduction correlates with reduced tissue damage. In particular, apoptosis is diminished in $GILZ^{TG}$ and this protective effect correlates with inhibition of Bax (a pro-apoptotic molecule) and with an increase of Bcl-2 (an anti-apoptotic molecule). Thus, GILZ over-expression contributes to reduce NO production and apoptosis.

Therefore, our results indicate that GILZ prevents SCI by 5 main mechanisms, such as: 1) inhibition of NF-κB activation, 2) prevention of T-cell activation, 3) decrease of Th2 cytokines production, 4) inhibition of T cells/neutrophils infiltration into the target tissue, and 5) inhibition of cytotoxic factors and tissue cell apoptosis.

Our observations, beyond the GILZ effect, indicate T lymphocytes are important cells in regulating the inflammatory process in SCI, and this may be a general phenomenon characteristic of most inflammatory/autoimmune diseases. In fact, T cells have a high regulatory capability in terms of stimulation and/or inhibition of soluble factors production, inflammatory cells recruitment, and permanence in the inflammatory lesion. Furthermore, T lymphocytes are important not only for disease development but also for immunological memory and disease maintenance. As is the case of most autoimmune/inflammatory disorders, T lymphocyte inhibition may well be of therapeutic value in the attempt to eradicate chronic inflammatory diseases.

In conclusion, results described herein demonstrate that GILZ (a mediator of GC anti-inflammatory activity) has a critical role in regulation of SCI development. Moreover,

these observations further indicate CD4+ and CD8α + T cells are important in SCI development and should represent an appropriate target for new therapeutic approaches. Evaluation of GILZ expression in T lymphocytes (during pharmacological therapy with GC) could be a mean to monitor the drug response and therapy outcome of autoimmune/inflammatory diseases.

Acknowledgments This work was supported by a research grant from the Italian Association for Cancer Research (AIRC) in Milan, Italy.

Required Author Forms Disclosure forms provided by the authors are available with the online version of this article.

References

1. Malmberg AB, Yaksh TL. Cyclooxygenase inhibition and the spinal release of prostaglandin E2 and amino acids evoked by paw formalin injection: a microdialysis study in unanesthetized rats. J Neurosci 1995;15:2768–2776.
2. Bartholdi D, Schwab ME. Methylprednisolone inhibits early inflammatory processes but not ischemic cell death after experimental spinal cord lesion in the rat. Brain Res 1995;672:177–186.
3. Amar AP, Levy ML. Pathogenesis and pharmacological strategies for mitigating secondary damage in acute spinal cord injury. Neurosurgery 1999;44:1027–1040.
4. Carlson SL, Parrish ME, Springer JE, Doty K, Dossett L. Acute inflammatory response in spinal cord following impact injury. Exp Neurol 1998;151:77–88.
5. de Castro R Jr, Hughes MG, Xu GY, et al. Evidence that infiltrating neutrophils do not release reactive oxygen species in the site of spinal cord injury. Exp Neurol 2004;190:414–424.
6. Gomez-Nicola D, Valle-Argos B, Suardiaz M, Taylor JS, Nieto-Sampedro M. Role of IL-15 in spinal cord and sciatic nerve after chronic constriction injury: regulation of macrophage and T-cell infiltration. J Neurochem 2008;107:1741–1752.
7. Popovich PG, Wei P, Stokes BT. Cellular inflammatory response after spinal cord injury in Sprague-Dawley and Lewis rats. J Comp Neurol 1997;377:443–464.
8. Profyris C, Cheema SS, Zang D, Azari MF, Boyle K, Petratos S. Degenerative and regenerative mechanisms governing spinal cord injury. Neurobiol Dis 2004;15:415–436.
9. Bracken MB, Shepard MJ, Holford TR, et al. Administration of methylprednisolone for 24 or 48 hours or tirilazad mesylate for 48 hours in the treatment of acute spinal cord injury. Results of the Third National Acute Spinal Cord Injury Randomized Controlled Trial. National Acute Spinal Cord Injury Study. JAMA 1997;277:1597–1604.
10. Hall ED. Antioxidant therapies for acute spinal cord injury. Neurotherapeutics 2011;8:152–167.
11. Lee JM, Yan P, Xiao Q et al. Methylprednisolone protects oligodendrocytes but not neurons after spinal cord injury. J Neurosci 2008;28:3141–3149.
12. Pott Godoy MC, Tarelli R, Ferrari CC, Sarchi MI, Pitossi FJ. Central and systemic IL-1 exacerbates neurodegeneration and motor symptoms in a model of Parkinson's disease. Brain 2008;131(pt 7):1880–1894
13. Rhen T, Cidlowski JA. Antiinflammatory action of glucocorticoids–new mechanisms for old drugs. N Engl J Med 2005;353:1711–1723.
14. Riccardi C, Bruscoli S, Migliorati G. Molecular mechanisms of immunomodulatory activity of glucocorticoids. Pharmacol Res 2002;45:361–368.
15. D'Adamio F, Zollo O, Moraca R et al. A new dexamethasone-induced gene of the leucine zipper family protects T lymphocytes from TCR/CD3-activated cell death. Immunity 1997;7:803–812.
16. Riccardi C, Bruscoli S, Ayroldi E, Agostini M, Migliorati G. GILZ, a glucocorticoid hormone induced gene, modulates T lymphocytes activation and death through interaction with NF-kB. Adv Exp Med Biol 2001;495:31–39.
17. Ayroldi E, Migliorati G, Bruscoli S et al. Modulation of T-cell activation by the glucocorticoid-induced leucine zipper factor via inhibition of nuclear factor kappa B. Blood 2001;98:743–753.
18. Berrebi D, Bruscoli S, Cohen N et al. Synthesis of glucocorticoid-induced leucine zipper (GILZ) by macrophages: an anti-inflammatory and immunosuppressive mechanism shared by glucocorticoids and IL-10. Blood 2003;101:29-738.
19. Bruscoli S, Donato V, Velardi E et al. Glucocorticoid-induced leucine zipper (GILZ) and long GILZ inhibit myogenic differentiation and mediate anti-myogenic effects of glucocorticoids. J Biol Chem 2010;285:10385–10396.
20. Cannarile L, Cuzzocrea S, Santucci L et al. Glucocorticoid-induced leucine zipper is protective in Th1-mediated models of colitis. Gastroenterology 2009;136:530–541.
21. Di Marco B, Massetti M, Bruscoli S et al. Glucocorticoid-induced leucine zipper (GILZ)/NF-kappaB interaction: role of GILZ homo-dimerization and C-terminal domain. Nucleic Acids Res 2007;35:517–528.
22. Ayroldi E, Zollo O, Bastianelli A et al. GILZ mediates the antiproliferative activity of glucocorticoids by negative regulation of Ras signaling. J Clin Invest 2007;117:1605–1615.
23. Ayroldi E, Riccardi C. Glucocorticoid-induced leucine zipper (GILZ): a new important mediator of glucocorticoid action. FASEB J 2009;23:3649–3658.
24. Cannarile L, Fallarino F, Agostini M et al. Increased GILZ expression in transgenic mice up-regulates Th-2 lymphokines. Blood 2006;107:1039–1047.
25. Delfino DV, Agostini M, Spinicelli S, Vito P, Riccardi C. Decrease of Bcl-xL and augmentation of thymocyte apoptosis in GILZ over-expressing transgenic mice. Blood 2004;104:4134–4141.
26. Genovese T, Rossi A, Mazzon E et al. Effects of zileuton and montelukast in mouse experimental spinal cord injury. Br J Pharmacol 2008;153:568–582.
27. Bethea JR, Castro M, Keane RW, Lee TT, Dietrich WD, Yezierski RP. Traumatic spinal cord injury induces nuclear factor-kappaB activation. J Neurosci 1998;18:3251–3260.
28. Shea TB. Technical report. An inexpensive densitometric analysis system using a Macintosh computer and a desktop scanner. Biotechniques 1994;16:1126–1128.
29. Ceruti S, Villa G, Genovese T, et al. The P2Y-like receptor GPR17 as a sensor of damage and a new potential target in spinal cord injury. Brain 2009;132(Pt 8):2206–2218.
30. McAndrew J, Patel RP, Jo H, et al. The interplay of nitric oxide and peroxynitrite with signal transduction pathways: implications for disease. Semin Perinatol 1997;21:351–366.
31. Xu J, Kim GM, Chen S et al. iNOS and nitrotyrosine expression after spinal cord injury. J Neurotrauma 2001;18:523–532.
32. Bal-Price A, Brown GC. Inflammatory neurodegeneration mediated by nitric oxide from activated glia-inhibiting neuronal respiration, causing glutamate release and excitotoxicity. J Neurosci 2001;21:6480–6491.
33. Madrigal JL, Moro MA, Lizasoain I et al. Inducible nitric oxide synthase expression in brain cortex after acute restraint stress is regulated by nuclear factor kappaB-mediated mechanisms. J Neurochem 2001;76:532–538.

34. La Rosa G, Cardali S, Genovese T, et al. Inhibition of the nuclear factor-kappaB activation with pyrrolidine dithiocarbamate attenuating inflammation and oxidative stress after experimental spinal cord trauma in rats. J Neurosurg Spine 2004;1: 311–321.
35. Fleming JC, Norenberg MD, Ramsay DA et al. The cellular inflammatory response in human spinal cords after injury. Brain 2006;129(Pt 12):3249–3269.
36. Vanegas H, Schaible HG. Prostaglandins and cyclooxygenases [correction of cycloxygenases] in the spinal cord. Prog Neurobiol, 64(4), 327–363 (2001).
37. Beaulieu E, Ngo D, Santos L et al. Glucocorticoid-induced leucine zipper is an endogenous antiinflammatory mediator in arthritis. Arthritis Rheum 2010;62:2651–2661.
38. Yang N, Zhang W, Shi XM. Glucocorticoid-induced leucine zipper (GILZ) mediates glucocorticoid action and inhibits inflammatory cytokine-induced COX-2 expression. J Cell Biochem 2008;103:1760–1771.
39. Verma IM. Nuclear factor (NF)-kappaB proteins: therapeutic targets. Ann Rheum Dis 2004;63(suppl 2):ii57-ii61.
40. Schwab ME, Bartholdi D. Degeneration and regeneration of axons in the lesioned spinal cord. Physiol Rev 1996;76:319–370.
41. Ahn YH, Lee G, Kang SK. Molecular insights of the injured lesions of rat spinal cords: Inflammation, apoptosis, and cell survival. Biochem Biophys Res Commun 2006;348:560–570.
42. Esposito E, Cuzzocrea S. Anti-TNF therapy in the injured spinal cord. Trends Pharmacol Sci 2011;32:107–115.
43. Nakamura M, Okada S, Toyama Y, Okano H. Role of IL-6 in spinal cord injury in a mouse model. Clin Rev Allergy Immunol 2005;28:197–204.
44. Cantarella G, Di Benedetto G, Scollo M et al. Neutralization of tumor necrosis factor-related apoptosis-inducing ligand reduces spinal cord injury damage in mice. Neuropsychopharmacology 2010;35:1302–1314.
45. Kwon BK, Tetzlaff W, Grauer JN, Beiner J, Vaccaro AR. Pathophysiology and pharmacologic treatment of acute spinal cord injury. Spine J 2004;4:451–464.
46. Nesic O, Xu GY, McAdoo D, High KW, Hulsebosch C, Perez-Pol R. IL-1 receptor antagonist prevents apoptosis and caspase-3 activation after spinal cord injury. J Neurotrauma 2001;18:947–956.
47. Dong H, Fazzaro A, Xiang C, Korsmeyer SJ, Jacquin MF, McDonald JW. Enhanced oligodendrocyte survival after spinal cord injury in Bax-deficient mice and mice with delayed Wallerian degeneration. J Neurosci 2003;23:8682–8691.